Carbon 154 (2019) 140–149

Contents lists available at ScienceDirect

Carbon

journal homepage: www.elsevier.com/locate/carbon

Theoretical investigations on stable structures of $C_{60-n}N_n$ (n=2–12): Symmetry, model interaction, and global optimization

Yun-Hua Cheng [a], Ji-Hai Liao [a], Yu-Jun Zhao [a, b], Jun Ni [c], Xiao-Bao Yang [a, b, *]

[a] Department of Physics, South China University of Technology, Guangzhou, 510640, People's Republic of China
[b] Key Laboratory of Advanced Energy Storage Materials of Guangdong Province, South China University of Technology, Guangzhou, 510640, People's Republic of China
[c] State Key Laboratory of Low-Dimensional Quantum Physics, Department of Physics, Tsinghua University, Beijing, 100084, People's Republic of China

ARTICLE INFO

Article history:
Received 29 May 2019
Received in revised form
20 July 2019
Accepted 26 July 2019
Available online 27 July 2019

ABSTRACT

Combining the extended cluster expansion method and the first-principles calculations, we have systematically investigated the structural stabilities of nitrogen doped C_{60} fullerene. With the structural recognition, we have calculated all possible isomers of $C_{60-n}N_n$ (n = 1–4) to obtain their ground state structures using the first-principles method. For $C_{60-n}N_n$ (n = 5–9) heterofullerenes, we have estimated the energy by the extended cluster expansion method to screen the candidates efficiently, followed by first-principles confirmation for the low-lying structures. For $C_{60-n}N_n$ with more than 9 nitrogen atoms, we developed a classification method to select the candidates and successfully obtained the low-lying isomers. The most stable structures for $C_{60-n}N_n$ (n = 3–11) we obtained have lower energies compared to the structures in previous studies. Notably, we have found 26 low-lying structures of $C_{48}N_{12}$ azafullerenes, from their 11.6 billion isomers.

1. Introduction

Heterofullerenes are fullerenes in which one or more carbon atoms that form the cage structures are replaced by non-carbon atoms, *i.e.*, heteroatoms. Because of the significant perturbations introduced by the heteroatoms, heterofullerenes exhibit a variety of novel properties leading to diversity of potential applications [1], *e.g.*, catalysts in hydrogenation reactions [2,3], nonlinear optical materials [4,5], and donor-acceptor pair for molecular electronics [6,7]. The first reported heterofullerenes were from the spectroscopic observation of gas-phase formation of boron doped fullerene, termed hereafter as borafullerenes [8]. Soon thereafter, spectroscopic evidences for gas-phase of various heterofullerenes were found by different groups [9–12]. Among all heterofullerenes, the $C_{60-x}N_x$ azafullerenes have been by far the most studied heterofullerenes. Hummelen et al. accomplished the first synthesis of heterofullerene ion $C_{59}N^+$ and biazafullerenyl $(C_{59}N)_2$ [13]. Replacement by an odd number of heteroatoms leads to radicals which can be stabilized by dimerization, whereas the substitution of an even number of C atoms would directly result in closed-shell structures [14]. Notably, a fullerene-like structure consisting of cross-linked nano-onions of $C_{48}N_{12}$ was synthesized, the core shell of which contains up to 20% N in composition [15].

It is still a challenge to investigate the heterofullerenes due to the numerous isomers. For heterofullerenes with higher heteroatom concentration, Shakib et al. calculated $C_{36}X_{24}$(X = Si, B, Al, N, and P) heterofullerenes with the T_h symmetry, where the dopants prefer to be isolated to avoid the weak hetero–hetero bonds [16]. Considering different isomers, Srinivasu et al. calculated electronic structure, stability and non-linear optical properties of azafullerenes $C_{60-2n}N_{2n}$(n = 1–12) and proposed the possible minimum energy structures for azafullerenes [17]. Chen et al. investigated several geometries of azafullerene to search the ground states of $C_{60-2n}X_{2n}$(X = N, B; n = 1–4) and $C_{70-2n}X_{2n}$(X = N, B; n = 1–5) [18,19]. Sharma et al. proposed the ground state structures for $C_{60-n}N_n$ for n = 1–12 by screening the specific structures using DFT calculations [20]. Garg et al. obtained the minimum energy structures of $C_{60-n}B_n$ by calculating the specific geometries [21].

A research hotspot of multi-nitrogen doped fullerenes is the $C_{48}N_{12}$ dodeca-azafullerenes [4,22–31]. The ground state structure of $C_{58}N_2$ indicates that the substitution of the para positions of hexagons is energetically preferable. Enlightened by this

* Corresponding author. Department of Physics, South China University of Technology, Guangzhou, 510640, People's Republic of China.
E-mail address: scxbyang@scut.edu.cn (X.-B. Yang).

https://doi.org/10.1016/j.carbon.2019.07.086
0008-6223/

characteristic, Hultman et al. succeeded in predicting a low-lying structure of $C_{48}N_{12}$ with one N per pentagon and S_6 point group symmetry [32]. In the next year, Manaa et al. theoretically predicted another structure of $C_{48}N_{12}$ with the same symmetry group [33]. In both the isomers, all nitrogen atoms disperse to the greatest extent since each pentagon has one nitrogen atom, and each nitrogen atom has a counterpart at one of its para positions. Unlike Hultman's structure which possesses the minimum separation of two carbon atoms between the nitrogen atoms, each nitrogen atom in Manaa's structure has another counterpart isolated by only one carbon atom. It was found that Manaa's isomer is more stable than the one found by Hultman, with 0.57 eV lower in the total energy, and 0.97 eV higher in the HOMO-LUMO gap, than those of Hultman's structure, respectively, indicating its potential applications in semiconductor device [33].

As is known, azafullerenes usually remain the perfect geometries of fullerenes [18,34]. The stabilities of heterofullerene depend on the substituted positions, therefore it is necessary to consider the possible isomers with specific number (n) of heteroatoms to search the minimum energy structure of $C_{60-n}N_n$. Among the 23 isomers of $C_{58}N_2$, the most stable $C_{58}N_2$ was found to have two nitrogen atoms at the para-positions of one hexagon in the previous studies [17,18,20,34]. Unlike the aggregation trend of boron heteroatoms [35], the stabilities of azafullerenes can be enhanced by dispersing the repulsive nitrogen atoms [33]. This characteristic may lead to highly doped fullerenes which remains the perfect geometry of C_{60} fullerene. However, the number of $C_{60-n}X_n$ isomers grows exponentially with the number of heteroatoms increasing [36]. All the previous studies were only based on the small number of specific candidates which were particularly chosen.

On the other hand, the charge state and spin multiplicity of molecules may also affect their structural stabilities and properties [37–39]. Wang et al. reported that the dependence of stability of endohedral metallofullerenes on the motifs varies with the charge state [40]. Considering various charges and spin configurations, M. Castro et al. investigated comprehensively the stability of C_{60}-like boron carbide fullerenes and carbon nitride fullerenes and found their anions behave as semi-metallic and magnetic nanomaterials. E. Chigo Anota et al. studied the neutral boron nitride cage, and found it has no magnetism and possesses a high chemical stability [41,42].

In this paper, we aim to search the ground state structures of $C_{60-n}N_n$ heterofullerenes for n = 2–12, based on the first-principles calculations combined with the extended cluster expansion (ExCE) and structural classification methods. For those low-lying structures, their stabilities are investigated with various charge states and possible spin multiplicities.

2. Computational methods

We perform the first-principles calculations for azafullerenes by the Vienna *Ab initio* Simulation Package (VASP) based on the density functional theory (DFT) [43–45]. The projector augmented wave (PAW) method and the Perdew Burke Ernzerhof (PBE) of generalized gradient approximation (GGA) are adopted as the pseudopotential method and correlation exchange functional [46,47], respectively, to calculate the total energy of all the considered heterofullerenes isomers. Structures are optimized using conjugate gradient algorithm and the residual forces are less than 0.02 eV/Å. A simple cubic shell of 20 Å is adopted to avoid any significant spurious interactions with periodically repeated images and the plane wave cutoff energy is set to be 520 eV.

The analysis for the structural stability is concerned with the commonly used quantum descriptors in DFT framework. Based on the calculated total energy, the cohesion energy is defined as follows [41],

$$E_{coh} = \left[E_{C_{60-n}N_n} - (60-n)E_C - nE_N\right]/60 \quad (1)$$

where $E_{C_{60-n}N_n}$ represents the total energy of a molecule of $C_{60-n}N_n$, E_C and E_N are the total energy of a single carbon atom and nitrogen atom, respectively. We also investigate the energy of the highest occupied molecular orbital (HOMO), the lowest unoccupied molecular orbital (LUMO) and the electronic energy gap, *i.e.*, HOMO-LUMO gap, defined as the difference of LUMO energy minus HOMO energy.

The structures of C_{60} and $C_{59}N$ are both unique, easily adopted to verify the accuracy of the calculations. The HOMO-LUMO gaps for C_{60} and $C_{59}N$ are calculated to be 1.64eV and 0.26eV, respectively. In $C_{59}N$, the two C-N bonds shared by pentagons and hexagons are both 1.42 Å, which is 0.03 Å shorter than their primitive length in C_{60} cage, but the edge shared by two hexagons almost remains the same length. All these calculations agree with those results reported in literatures [6,48–50].

For multi-azafullerenes, the stabilities of isomers are obviously dependent on the relative positions of the heteroatoms. According to numbering scheme proposed by IUPAC [51], we have proposed a congruence check method [52], where the minimal structure index (MSI) denotes a unique heterofullerene isomer. Note that the number of isomers grows exponentially with the number of heteroatoms increasing, *e.g.*, the $C_{58}N_2$, $C_{57}N_3$, $C_{56}N_4$ heterofullerenes have 23, 303, 4190 isomers, respectively, while there are 21,330,558 isomers of $C_{52}N_8$, and for $C_{48}N_{12}$, the astronomical number is 11,661,527,055.

Thus, we have calculated all possible isomers of $C_{60-n}N_n$ (n = 2–4) to obtain the ground state structures using the first-principles method. For $C_{60-n}N_n$ (n = 5–9) heterofullerenes, we have estimated the energy by the ExCE method to screen the candidates efficiently, where the low-lying structures are further confirmed by the first-principles calculations. For $C_{60-n}N_n$ with more than 9 nitrogen atoms, we developed a classification method to select the candidates and successfully obtained the low-lying structures. The schematic flow chart of our computational methods is shown in Fig. 1.

For a certain nitrogen concentration, each of the obtained low-lying structures has three forms: neutrals, cations and anions. Besides the neutral one, we further investigate 2 types of charged molecules: $(C_{60-n}N_n)^+$ and $(C_{60-n}N_n)^-$ with the spin multiplicity $M = 2S_T + 1$, where S_T is the total spin of the valence electrons. For even number of electrons, spin multiplicity, if restrained no more than 6, has 3 types of values: 1, 3 and 5, and for odd number of electrons, the values are 2, 4 and 6. Therefore there are 9 configurations of charge state and spin multiplicity in all for each considered isomer. Because of the different chemical potentials introduced by different numbers of electrons [53], we could not directly compare their relative energy to rank their relative stability, unless the electron numbers are the same. In fact, more electrons introduced in anions, the coulomb potential energy between nuclei and electrons will decreases, which may lead to a reduction in the total energy of the system [54], *e.g.* $(C_{60})^-$ anion has more lower energy than neutral C_{60} [55]. Therefore, a lower energy state may not be more stable since it has a different charge state. The calculated results are shown for two most stable isomers of $C_{58}N_2$ in Table S1. (1, 7) is the most stable structure of neutral $C_{58}N_2$. For $(C_{60-n}N_n)^-$, (1, 7) keeps more stable than (1, 41), but for $(C_{60-n}N_n)^+$, (1, 41) turns energetically preferable. Spin multiplicity always tends to take the minimum, 1 or 2, depending on the parity of the number of electrons.

A stable structure must be at the point where the potential energy surface (PES) has a local minimal value, and the vibrations of

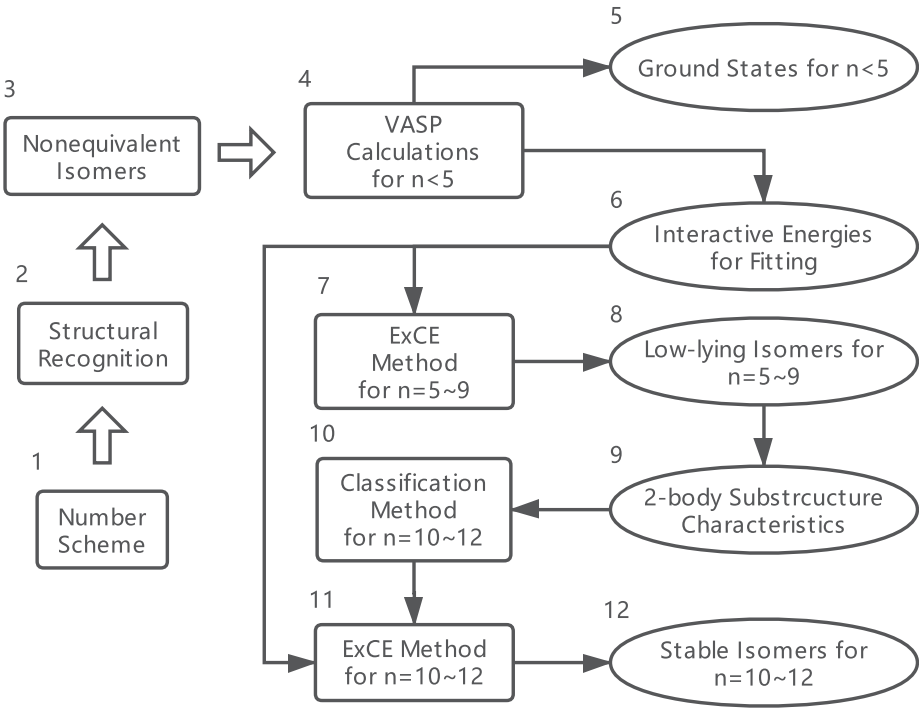

Fig. 1. The schematic flow chart of the structural screening. The first 3 steps make the enumeration for the isomers. In the 4th ~6th steps, the ground states of $C_{60-n}N_n$ for n = 2–4 and the interactive energies to be used for fitting in the ExCE method are obtained using first-principles method. In the 7th~9th steps, the ExCE method is combined with DFT calculations to obtain the low-lying isomers of $C_{60-n}N_n$ for n = 5–9, and the 2-body substructures of the $C_{60-n}N_n$ (n = 5–9) isomers with higher stability are investigated. In the 10th~12th steps, the classification method is employed to filter out the majority of the isomers with low stability and the ExCE method is adopted to predict the stability of the remained isomers, leading to the most stable isomers of $C_{60-n}N_n$ for n = 10–12.

all degrees of freedom should not have imaginary frequencies [56,57]. We have checked all the obtained low energy structures and all frequencies are positive, indicating the stabilities of all our obtained low-lying structures. On the other hand, The energy calculated by DFT only determines the stability of a heterofullerene structure at $T = 0$ K [58]. At finite temperature, the entropy contribution to free energy should be also considered. To avoid the large time-consuming calculation by molecular dynamics (MD) method, Gibbs free energy (GFE) for different temperature can be calculated by the resonance approximation formula as below [59],

$$F = E_0 + \sum_i \hbar\omega_i/2 + kT\sum_i ln[1 - exp(-\hbar\omega_i/kT)] \quad (2)$$

where E_0 is the total energy of the structure at temperature of absolute zero. ω_i is one of the vibrational frequencies of the molecule. Since C_{60} azafullerene molecule has 60 atoms in total, there are $3 \times 60 - 6 = 174$ vibrational frequencies.

3. Results and discussions

With the congruence check based on the MSI for heterofullerenes, we have screened the nonequivalent isomers of $C_{60-n}N_n$ for n = 2–12 to search the stable structures of azafullerenes with different nitrogen concentration. In Sec. 3.1, the ground states of $C_{60-n}N_n$ for n = 2–4 are reported, and the most stable structures of $C_{60-n}N_n$ for n = 5–9 are presented and the structural characteristics are discussed. In Sec. 3.2, we propose a classification method to screen efficiently the isomers of azafullerenes with more than 9 nitrogen atoms. In Sec. 3.3, the most stable structures of $C_{60-n}N_n$ for n = 10–12 are presented, and the obtained isomers of dodecaazafullerenes $C_{48}N_{12}$ are intensively investigated.

3.1. Low-lying isomers of $C_{60-n}N_n$ for n = 2–9

Based on the structure recognition method for heterofullerenes [52], we have performed the first-principles calculations for all the nonequivalent isomers of $C_{60-n}N_n$ (n = 2–4) to obtain the minimal energy structures, which are shown in Fig. 2a–c. The most stable $C_{58}N_2$ agrees with the one from literatures [17,18], where two nitrogen atoms are at the para positions of a hexagon. Its HOMO-LUMO gap is found to be 0.64eV, which is in good agreement with the reported values [17,60]. We found that the minimum energy isomer of $C_{57}N_3$ denoted by (1, 41, 48), which has C_{3v} symmetry, is the most highly symmetrical cage among all the 303 triazafullerenes isomers. The most stable structure of $C_{56}N_4$ is found to be (1, 7, 28, 35). As shown in Table 1, the ground states of $C_{57}N_3$ and $C_{56}N_4$ by our enumeration have lower energies than those found in the previous studies [17,18,20].

In our previous work [52], we proposed the ExCE method for $C_{60-n}B_n$ (n > 4), where an isomer of heterofullerene is described by its substructures. Based on the first-principles calculations, we obtain the interactive energies of all possible substructures of $C_{60-n}B_n$ (n = 2–4) by linear regression algorithm, which are then combined linearly to predict the energy of those heterofullerenes with higher heteroatom concentration. The substructures with the same number of heteroatoms share the same fitting coefficient, *i.e.*, the concentration dependent fitting. With more structures calculated, the fitting coefficients are adjusted, and the errors approach normal distribution. When the number of low-lying structures converges, we then obtain the low-lying structures for various heteroatom concentrations.

Using the ExCE model, we have performed a thorough screening for the azafullerenes with 5–9 nitrogen heteroatoms and obtained the most stable structures so far. We first obtain the model

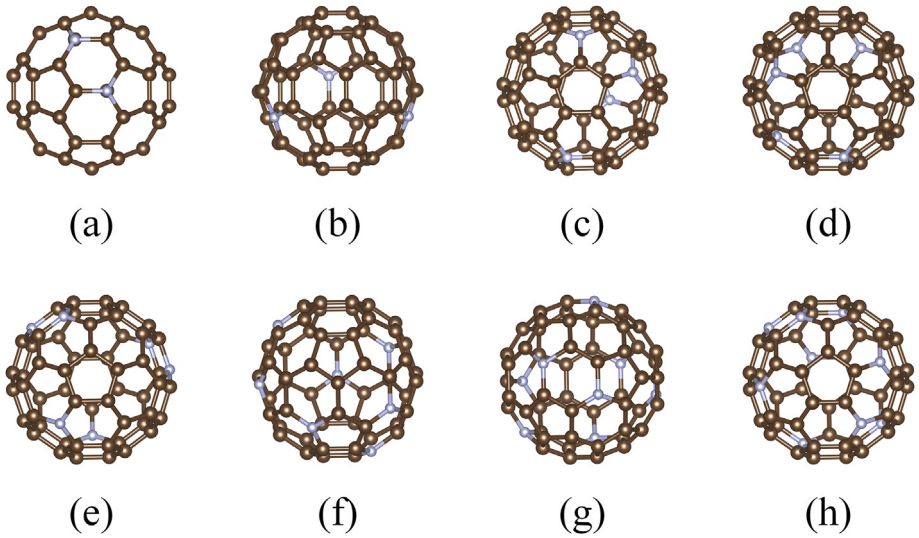

Fig. 2. The most stable isomers of $C_{60-n}N_n$ (n = 2–9). The ground states of $C_{58}N_2$, $C_{57}N_3$ and $C_{56}N_4$ are shown in (a), (b) and (c), respectively. The obtained most stable structures of $C_{55}N_5$, $C_{54}N_6$, $C_{53}N_7$, $C_{52}N_8$ and $C_{51}N_9$ are shown in (d), (e), (f), (g) and (h), respectively. The MSIs of these isomers are listed accordingly in Table 1. (A colour version of this figure can be viewed online.)

Table 1
The most stable isomers of $C_{60-n}N_n$ for n = 2–11, compared with those reported in literatures.ΔE (unit is eV) is defined as the energy of the isomer reported previously relative to that of the counterpart we obtained. For $C_{60-n}N_n$ (n = 3–11), the isomers proposed by our study have higher stability.

n	Our result	Reported previously	ΔE
2	(1,7)	(1,7) [17,18]	0.00
3	(1,41,48)	(1,14,17) [20]	0.29
4	(1,7,28,35)	(1,7,11,24) [17,18,20]	0.62
5	(1,7,29,34,59)	(1,14,17,24,58) [17,20]	0.32
6	(1,7,28,34,37,56)	(1,6,11,16,18,36) [18]	0.23
		(1,6,11,18,27,31) [20]	0.25
		(1,7,11,14,24,27) [17]	0.10
7	(1,7,15,32,35,45,57)	(1,13,16,22,28,44,53) [20]	0.35
8	(1,7,16,19,31,36,45,57)	(1,6,11,16,18,24,27,36) [18]	0.16
		(1,7,13,18,26,36,43,50) [20]	0.39
		(1,7,11,24,27,34,37,50) [17]	0.44
9	(1,7,14,17,26,44,47,52,55)	(1,7,13,18,26,36,43,46,50) [20]	0.25
10	(1,7,14,17,26,35,44,47,54,60)	(1,7,13,18,26,36,43,46,50,60) [20]	0.25
		(1,7,11,24,27,34,37,50,54,60) [17]	0.07
11	(1,6,11,18,23,27,33,40,48,51,58)	(1,3,7,19,26,30,36,40,44,50,60) [20]	0.25

coefficients by fitting the first-principles calculations of the randomly selected structures, then we intensively screen those isomers with the lowest predicted energy. For $C_{54}N_6$, $C_{53}N_7$ and $C_{52}N_8$ azafullerenes, the screening results are shown in Fig. 3, where the relations between the relative energies from first-principles calculations and those from ExCE method are plotted.

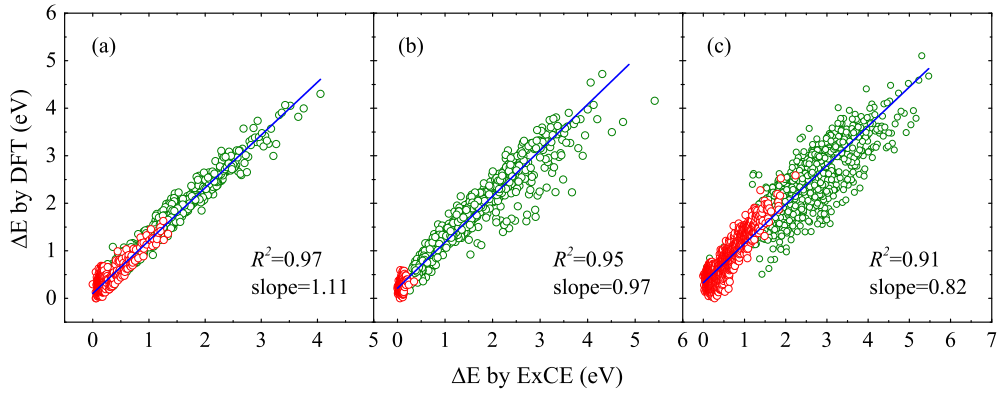

Fig. 3. The VASP calculated energy versus that from ExCE method. The data of $C_{54}N_6$, $C_{53}N_7$ and $C_{52}N_8$ are shown in (a), (b) and (c), respectively. The randomly selected structures and the more stable structures predicted by the ExCE model are represented by green and red circles, respectively. ΔE by VASP and ExCE are the energies relative to the minimal energies obtained by VASP and ExCE, respectively. For each nitrogen concentration, the linear fitting is done for all the data. (A colour version of this figure can be viewed online.)

For $C_{54}N_6$ and $C_{53}N_7$, the correlation coefficient (R^2) is more than 0.95 and the slope is very close to 1, and for $C_{52}N_8$, the correlation is still good ($R^2 = 0.91$), showing a very good consistency between the first-principles method and the ExCE method, indicating the high reliability of prediction by the ExCE method. The ground state structures of $C_{60-n}N_n$ for n = 5–9 are shown in Fig. 2d–h. As shown in Table 1, all these low-lying structures have lower energies compared to the corresponding structures of azafullerenes in previous studies [17,18,20]. On the other hand, compared to the long range of the randomly selected isomers, the screened isomers with low predicted energy distribute in a rather small low-energy region, hence the ExCE mothed can easily filter out the majority of the isomers with low stability and provides a high efficiency in structural screening.

For all these obtained low-lying structures, three charge states are considered, and for each charge state, three spin configurations are investigated. All the most stable structures of various charge states are listed in Table S2. For $C_{48}N_{12}$, the most stable structures of three charge states are different from each other. For other cases, the lowest energy structure for the anion or cation is the minimal energy structure of neutral molecule. But spin multiplicity of any stable structure is 1 or 2, decided by the number of electrons.

In order to confirm the stability of low-lying structures and consider the temperature effect, the vibrational calculations were performed for the low-lying structures of various nitrogen concentration. All the 174 vibrational frequencies are found to be positive for any structure we checked. GFE is defined by Eq. (2). For a certain azafullerene formula, The GFE versus temperature for the 10 lowest energy isomers of $C_{58}N_2$ are shown in Fig. 4a. Similar results with various nitrogen numbers are shown in Fig. S4 in the supplementary information. These results indicate that for various nitrogen concentration, the most stable structure at 0 K is always the lowest energy structure in the temperature range of 0–300 K.

Among the 23 isomers of the $C_{58}N_2$ azafullerenes (shown in Fig. S1 in the supplementary material), (1, 7), (1, 42) and (1, 23) are the three most stable isomers while (1, 2), (1, 9), (1, 3) and (1, 6) are the isomers with highest energy. Nitrogen atoms in the (1, 2) and (1, 9) isomers are at the ortho positions of pentagons and hexagons respectively, and two nitrogen atoms in the (1, 3) and (1, 6) structures are isolated by one carbon atom. To study the effect of 2-body substructures on the azafullerenes' stability, we make a statistic for the 23 2-body substructures in the obtained more stable structures of $C_{60-n}N_n$ for n = 3–9. We select 100 isomers with the lowest energy for each heteroatom concentration and count the contained 2-body substructures accordingly. In Fig. 5, the counts of all 2-body substructures are shown ordered by the increasing energies of

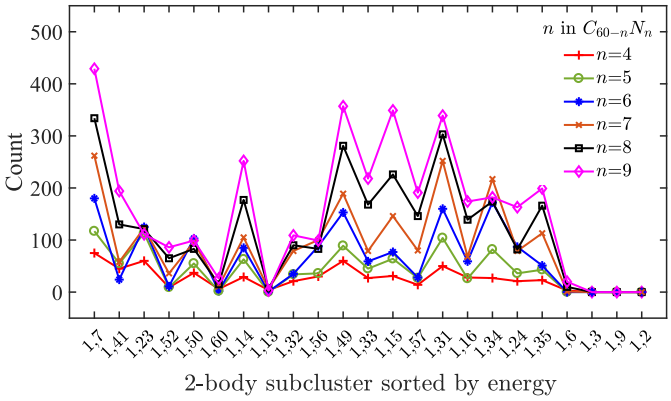

Fig. 5. The counts of the 2-body substructures in the 100 isomers with the lowest energy for each heteroatom concentration. The 2-body substructures are sorted by the energies of the corresponding $C_{58}N_2$ isomers. (A colour version of this figure can be viewed online.)

the $C_{58}N_2$ isomers. The proportions of the 2-body substructures vary as a function of the nitrogen concentration, where the change trends of the proportions are essentially consistent. Among all the 2-body substructures, (1,7) has the highest proportion, (1,49), (1,15) and (1,31) also have important contributions to the stabilities of the structures. On the other hand, the proportions of (1,9), (1,2), (1,3) and (1,6) are almost zero, indicating that the azafullerenes will be unstable if there are nitrogen atoms adjacent to each other or isolated by one carbon atom.

3.2. Classification of $C_{60-n}N_n$ for n = 10–12

With the number of nitrogen atoms getting more than 9, the numbers of isomers become over huge for the direct usage of ExCE method. To avoid this matter, we propose a classification method to filter out the isomers of low stabilities. In fact, from the above statistics of 2-body substructures, nitrogen atoms in azafullerenes could not be neighbors or isolated by one carbon atom, otherwise, the total energies of the isomers will be relatively high. We gradually reduce the number of those isomers by adding the restrictions, which are listed in Table 2. Firstly, we exclude the isomers containing more than two heteroatoms on any pentagon or hexagon, the numbers of the rest of the nonequivalent isomers are listed in the column titled by R_1. On the base of R_1, we then remove the structures which contain more than one nitrogen atom on any pentagon, resulting the R_2 column. Further, we remove all the

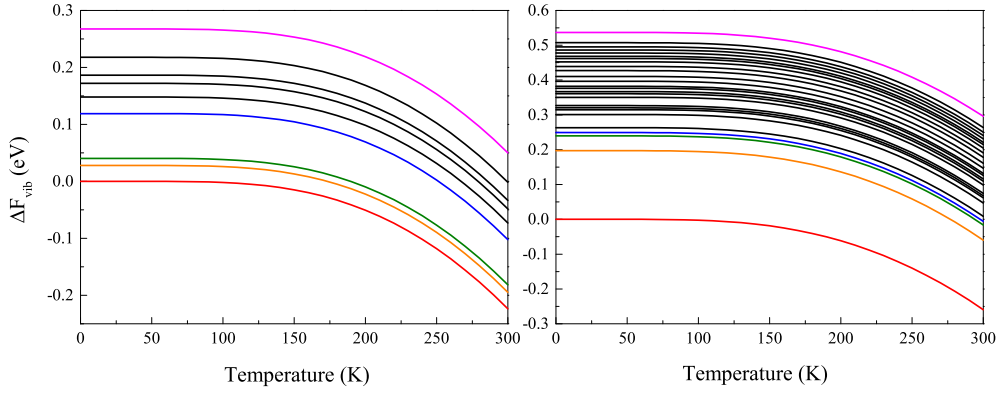

Fig. 4. The GFE versus temperature for (a) 10 lowest energy isomers of $C_{58}N_2$ and (b) 26 lowest energy isomers of $C_{48}N_{12}$. ΔF_{vib} is defined as the calculated GFE minus the minimal GFE at T = 0. In both panels, red, orange, green and blue line represents the 1st, 2nd, 3rd, 4th lowest energy neutral isomer, respectively. The pink lines represent the 10th, 26th lowest energy isomer for $C_{58}N_2$ and $C_{48}N_{12}$, respectively. Other intermediate isomers are shown in black lines. (A colour version of this figure can be viewed online.)

Table 2
The numbers of nonequivalent isomers under different screening conditions.

n	R_0	R_1	R_2	R_3	R_4	R_5	R_6	R_7	R_8
1	1	1	1	1	1	1			
2	23	23	21	20	19	18	1	1	1
3	303	297	243	229	181	157			
4	4190	3955	2662	2365	1429	1058	18	14	15
5	45718	39791	20712	17040	6881	3892			
6	418470	320152	120850	89687	21144	8026	148	58	83
7	3220218	2038063	515950	336933	38719	7904			
8	21330558	10394687	1613050	902419	41301	3325	920	98	229
9	123204921	42423110	3581375	1667833	23362	411			
10	628330629	138141506	5374131	2020015	6321	14	2985	26	144
11	2855893755	355480910	4883125	1432314	608	0			
12	11661527055	712355058	2036775	449788	12	0	5008	2	10

isomers containing adjacent heteroatoms and obtain R_3 column. R_4 column retains the isomers where nitrogen atoms are not neighbors or isolated by one carbon atom. R_5 represents the isomers which have no more than one heteroatom on any ring. If we restrain that any nitrogen atom should have at least one counterpart at the para positions, we get the column titled by R_6. Removing the isomers in R_6 containing more than one nitrogen atom on any pentagon results in R_7 column. The last column titled by R_8 is the intersection of R_2 and R_6. Some examples of the classification method are given in the supplementary material.

After screening the structures of $C_{60-n}N_n$ (n = 5–9) in R_1 using ExCE method, the 100 lowest isomers obtained are almost the same as that from R_0, indicating that the screening condition of R_1 works well and the majority of the isomers with lower energies are found. But for the azafullerenes with more than 9 heteroatoms, the numbers of the rest of the isomers remain so enormous that the structural searching by ExCE method is still inefficient. Since any pentagon of the cage prefers no more than one nitrogen atom, lots of structures in R_1 are removed and R_2 is obtained where the numbers of azafullerenes with more than 9 nitrogen atoms get as small as mega level, which makes the ExCE method become practicable for any azafullerenes since only those structures with lower energies are retained. Compared to the calculations based on R_1, the root means square errors (RMSEs) of the fittings get smaller, which means the precision of fitting is improved. The most important finding of the screenings from R_2 is that we find more than 10 structures of $C_{48}N_{12}$ which have lower energies than that of the Hultman's structure.

From the statistics above, like pentagons, hexagon does not prefer to contain neighbor nitrogen atoms. Hence, we study the isomers from the list of R_3 using ExCE method. The numbers of structures become smaller compared to R_2, but the efficient for searching low-lying structures almost remains the same as that of R_2 because the filtered isomers with high energies are also predicted to be of low stabilities in the fittings for the list of R_2. We make a statistic for the average distances between the nitrogen atoms in all the calculated structures and find that those isomers with lower energies have larger distances compared to those of low stabilities. Considering that the fully relaxed geometries of azafullerenes almost maintain the perfect cage of C_{60} fullerene, we retain those $C_{48}N_{12}$ isomers from the list of R_3 if the average distance among nitrogen atoms in their initial unrelaxed cages is larger than 2.8 Å, which comes up to 30656 in total and is much smaller than that of R_3. By calculating hundreds of structures with low predicted energies, we obtain several low-lying structures whose energies are lower than that of Hultman's structure, especially the minimal energy structure ever found so far, *i.e.*, Manaa's structure, is also obtained. Considering the astronomical number of the isomers of $C_{48}N_{12}$, our global screening method shows a rather high efficiency for structure search. Since a nitrogen atom rarely has a counterpart at the meta-position on a hexagon, we further filter the isomers containing the substructures denoted by (1, 6) and obtain the structures in R_4, where there are only 12 $C_{48}N_{12}$ isomers. The Hultman's structure for $C_{48}N_{12}$ is found to be among the 12 isomers. But Manaa's structure is filtered out from the set since it has nitrogen atoms at meta-positions of hexagons.

Low-lying azafullerene structures containing aggregated nitrogen atoms are removed by the filtering rules from R_1 to R_4, indicating that the nitrogen atoms prefer to disperse on the cage. But substructures with large distance, on the other hand, are not always favorable for high concentration azafullerenes, for example, (1,60), (1,57) and (1,56) have smaller counts in the statistics of 2-body substructures though they have the largest average distance between their substituted vertices. Almost all azafullerenes isomers with more than one nitrogen atoms on any pentagon are not stable. For the hexagon, the nitrogen atoms at the para-positions are beneficial to the stability of the structure, while some structures with nitrogen atoms at the meta-positions also maintain high stability. The R_5 constraint is over restrict since too many structures with low energies have been filtered out.

From the statistics of 2-body interactions, the substructure of (1, 7) always has the highest proportion for all low-lying azafullerenes structures with different nitrogen concentrations, which is regarded as a significant characteristic. We call this characteristic as highest proportion of para positions. Considering isomers in which any nitrogen atom has a counterpart at the para position, we obtain isomers with the total numbers in R_6 column, for example, the total number of the isomers for $C_{48}N_{12}$ is 5008. After calculating for several hundreds of isomers which are predicted with lower energies, we obtain Hultman's and Manaa's structures of $C_{48}N_{12}$, and other 24 $C_{48}N_{12}$ isomers whose energies are between those of Hultman's and Manaa's structures are also found by our fitting method. Based on R_6, if removing all the isomers with heteroatoms at ortho and meta positions, we get R_7 column. In this set, only 2 $C_{48}N_{12}$ isomers are left, including Hultman's structure.

3.3. Low-lying isomers of $C_{60-n}N_n$ for n = 10–12

With the above classification, we have screened the stable structures of $C_{60-n}N_n$ (n = 10–11), as listed in Table 1. The ground state of $C_{50}N_{10}$ is (1, 7, 14, 17, 26, 35, 44, 47, 54, 60), as shown in Fig. 6a. The symmetry group of the structure is C_2. There are 4 substructures denoted by (1, 7). The isomer (1, 7, 11, 24, 27, 34, 37, 50, 54, 60) where the heteroatoms make up two pentagons on the two hemispheres, reported as ground state of $C_{50}N_{10}$ by Srinivasu et al. [17], has a 0.07 eV higher energy, thought it has a higher symmetry described by D_{5d}. Another stable $C_{50}N_{10}$ isomer (1, 7, 13, 18, 26, 36, 43, 46, 50, 60) reported in literature has a 0.25 eV higher

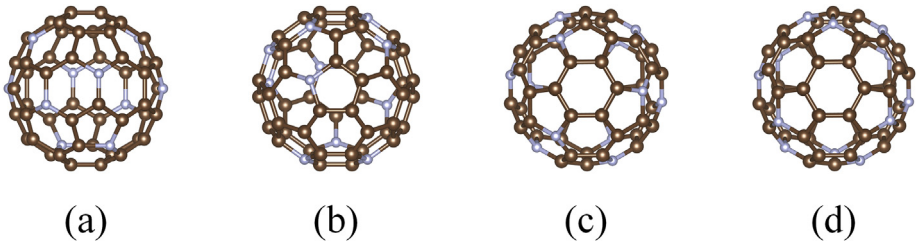

Fig. 6. Low-lying structures for $C_{60-n}N_n$ (n = 10–12). $C_{50}N_{10}$ and $C_{49}N_{11}$ are shown in (a) and (b), respectively. Manaa's and Hultman's structures for $C_{48}N_{12}$ are shown in (c) and (d), respectively. (A colour version of this figure can be viewed online.)

energy [20]. The minimal energy structure of $C_{49}N_{11}$ is (1, 6, 11, 18, 23, 27, 33, 40, 48, 51, 58) shown in Fig. 6b. The energy of this structure is 0.56 eV lower than the most stable structure reported by Sharma [20], which is denoted by (1, 3, 7, 19, 26, 30, 36, 40, 44, 50, 60).

For the intensively investigated $C_{48}N_{12}$ heterofullerenes, considering all the calculated isomers belong to R_2 list, we make a linear fitting between the DFT calculations and the ExCE predictions and then get the Pearson's correlation coefficient (0.93) and the Adj. R-Square (0.86), indicating there is a good consistency between the first-principles method and the ExCE method, as shown in Fig. 7a. Based on the classification method, our ExCE prediction model offers a high screening efficiency since all the screened structures predicted by ExCE are located in a narrow low-energy region, as show in Fig. 7b. Though we have calculated only about 3000 isomers, we managed to obtain the most stable isomers, despite the enormous number of the nonequivalent isomers of $C_{48}N_{12}$ which is over 11.6 billion.

We obtain the two most stable structures reported so far, Manaa's and Hultman's structures [15,33], shown in Fig. 6c and d, respectively, and other 24 remarkably stable structures (see cages shown in Fig. S3). The 26 isomers are listed in Table 3, where the energies are relative to that of the Manaa's structure denoted by (1, 6,11,16,18,26,36,44,46,49,54,60). For all the obtained isomers, their energies relative to that of Manaa's structure are shown in Fig. S3, which indicates that $C_{48}N_{12}$ has lots of isomers with very close stabilities. Among all the calculated isomers, Manaa's structure has the lowest energy, and it also has the highest HOMO-LUMO gap in the 26 remarkably stable structures, therefore we believe that Manaa's structure should be the ground state of $C_{48}N_{12}$.

For the chage states of $C_{48}N_{12}$, $(C_{48}N_{12})^+$ and $(C_{48}N_{12})^-$, we consider the 3 spin multiplicities (M = 2, 4 and 6) for each charge state. As the most stable structure of neutral $C_{48}N_{12}$, Manaa's structure has a considerable energy difference relative to the second lowest energy structure denoted by (1, 6, 8, 11, 16, 18, 23, 36, 46, 49, 54, 60). Note that (1, 6, 11, 15, 18, 23, 25, 31, 41, 45, 51, 57) becomes the lowest energy isomer when charge is −1, and (1, 6, 11, 15, 18, 26, 35, 44, 46, 49, 54, 60) is the most stable for cations, which is shown in Table S2.

For neutral molecules, Manaa's structure has a high thermal stability. As shown in Fig. 4b, the Manaa's structure (marked in red line) always keeps the highest stability in the temperature range of 0–300 K.

There are 11 kinds of 2-body substructures in Manaa's structure, including (1, 6), (1, 7), (1,15), (1, 16), (1, 23), (1, 31), (1, 33), (1, 35), (1, 49), (1, 50) and (1, 60). The occurring times of all the 2-body substructures are 6. Compare to the Hultman's isomer, the N-N repulsive interaction in Manaa's structure is outweighed and compensated by the stabilizing contribution of the local aromaticity in the eight all-carbon hexagonal rings, which is the driving force toward the maximum stability [33].

The HOMO-LUMO gap of Manaa's structure is not the highest one among all the calculated isomers, as shown in Fig. 8, where the relationship between the relative energy and HOMO-LUMO gap of calculated $C_{48}N_{12}$ isomers is plotted. An isomer denoted by (1, 6, 8, 16, 28, 30, 35, 37, 41, 43, 48, 56), as shown by the circled point in

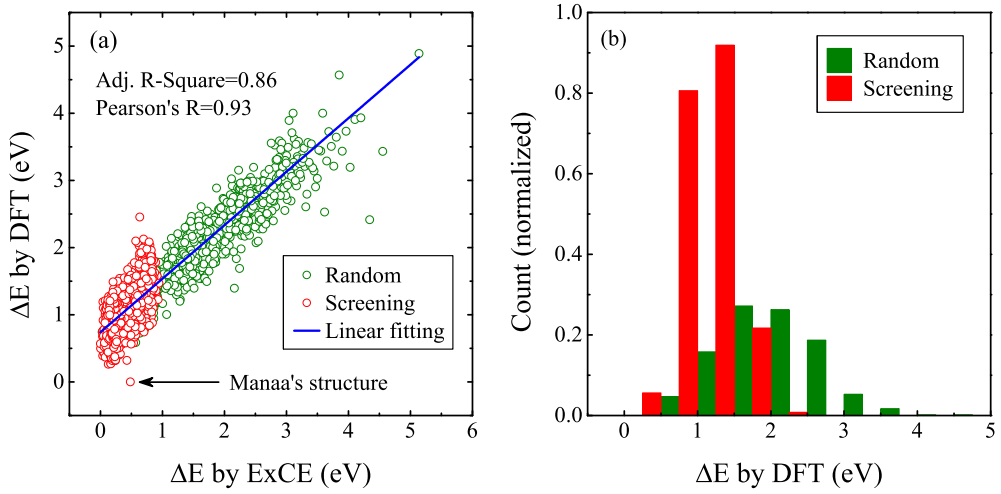

Fig. 7. The relative energy of the calculated isomers of $C_{48}N_{12}$. VASP calculated energy versus the energy predicted by the ExCE method is in (a), where the green and red circles represent the isomers randomly selected and the more stable structures predicted by the ExCE model, respectively. The linear fitting is done for all the data. In (b), the VASP calculated energies are counted for the randomly selected isomers and the screened isomers with low predicted energy, represented by green and red histogram, respectively. (A colour version of this figure can be viewed online.)

Table 3
The obtained 26 low-lying isomers of $C_{48}N_{12}$ azafullerenes. The relative energy, denoted by ΔE (unit is eV), is the energy of the isomer relative to that of the most stable one denoted by (1, 6,11,16,18,26,36,44,46,49,54,60).

MSI	ΔE	MSI	ΔE
1, 6,11,16,18,26,36,44,46,49,54,60	0	1, 6,11,18,23,25,33,41,45,48,51,57	0.270
1, 6, 8,11,16,18,23,36,46,49,54,60	0.168	1, 6,11,14,18,23,25,31,36,41,45,57	0.280
1, 6,11,15,18,26,35,44,46,49,54,60	0.195	1, 6,11,14,18,26,35,44,46,49,54,60	0.287
1, 6,11,15,18,26,36,44,46,49,54,60	0.196	1, 6,11,15,18,26,36,44,46,50,54,60	0.303
1, 6, 8,11,18,23,33,46,49,51,54,60	0.204	1, 6,11,18,23,25,34,36,39,45,50,57	0.305
1, 6,11,15,18,26,31,41,44,47,51,59	0.233	1, 6, 8,11,16,18,23,28,31,36,41,57	0.314
1, 6, 8,11,16,18,36,43,46,49,54,60	0.238	1, 6,11,15,18,25,27,32,35,39,42,56	0.316
1, 6,11,14,18,25,31,36,39,42,45,57	0.239	1, 6, 8,11,15,18,23,28,31,41,51,57	0.317
1, 6, 8,11,16,18,23,28,31,36,54,60	0.240	1, 6,12,15,18,23,25,31,41,45,51,57	0.318
1, 6,11,18,25,27,33,42,49,51,54,56	0.257	1, 6, 8,11,14,18,23,28,31,36,41,57	0.318
1, 6,11,14,18,23,25,31,36,39,45,57	0.264	1, 6, 8,11,15,18,23,28,31,35,54,60	0.319
1, 6,11,15,18,23,25,31,41,45,51,57	0.264	1, 6,11,15,18,26,31,39,44,47,51,59	0.319
1, 6, 8,11,14,18,23,28,31,35,54,60	0.269	1, 7,15,18,26,29,36,39,43,46,50,60	0.319

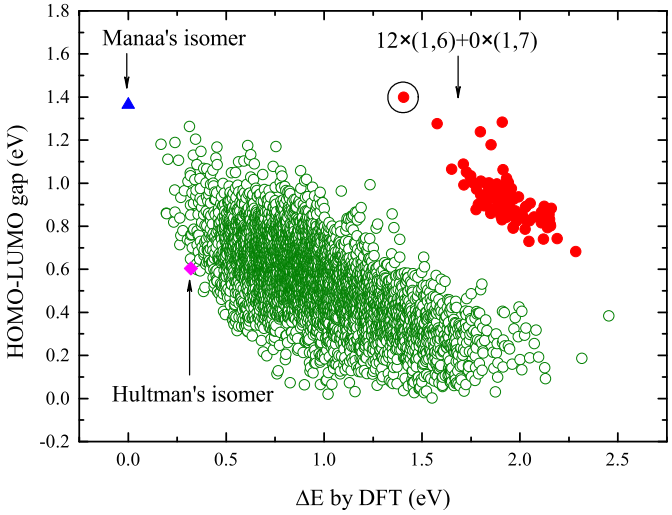

Fig. 8. The HOMO-LUMO gap versus stability of $C_{48}N_{12}$. The red points represent the isomers which have 12 nitrogen substituted meta positions and have not nitrogen atoms at para positions. The circled red point represents the isomer with the highest HOMO-LUMO gap. The blue triangle and pink diamond are the Manaa's structure and Hultman's structure, respectively. ΔE is the energy relative to that of the most stable isomer. (A colour version of this figure can be viewed online.)

Fig. 8, is found to have a higher HOMO-LUMO gap than that of Manaa's structure. The calculated isomers of $C_{48}N_{12}$ can be divided into 2 isolated regions. In both the regions, the HOMO-LUMO gap decreases roughly while the total energy becomes higher. In the region with higher HOMO-LUMO gap, all isomers have not nitrogen at para positions and there are 12 substructures of (1, 6). The stabilities of the isomers in this region are almost lower than those in the other region, therefore more nitrogen substitutions at meta positions may lead to lower stabilities.

So far, we have got the most stable structure of $C_{60-n}N_n$ for n = 2–12, of which the related calculated data are listed in Table 4. As mentioned above, for the obtained isomers of $C_{60-n}N_n$ (n = 2–12), nitrogen substitutions at para positions are important to maintain the stabilities of the structures. Apart from $C_{57}N_3$, all the obtained ground state structures or low-lying isomers of $C_{60-n}N_n$ for n = 2–12 have para positions substituted by nitrogen atoms. For the minimal energy structures of $C_{56}N_4$, $C_{54}N_6$, $C_{52}N_8$, $C_{50}N_{10}$ and $C_{48}N_{12}$, there are 1, 2, 3, 4 and 6 substructures denoted by (1, 7), respectively. Hence the number of substituted para positions increases as the nitrogen concentrations increase, which is shown in Fig. 9. On the other hand, for those $C_{48}N_{12}$ isomers with more than 6 para positional substitutions, the stabilities are all found to be very weak, hence more substituted para positions are not necessary for the stability of azafullerenes.

4. Conclusion

With the structural recognition, we have enumerated the ground structures of $C_{60-n}N_n$ for n < 5 by the first-principles calculations. It is found that in $C_{58}N_2$, the nitrogen atoms prefer to be at the para positions of a hexagon, while para positions are not energetically preferable for nitrogen in $C_{57}N_3$ and $C_{56}N_4$. We have used the ExCE method to search the low-lying structures of $C_{60-n}N_n$ for n = 5–9, where the predicted energies by the ExCE method are consistent with those from the first-principles calculations. For the

Table 4
The obtained lowest energy structures for neutral azafullerene molecule $C_{60-n}N_n$ for n = 2–12. Data of $C_{59}N$ and C_{60} are attached for the sake of comparison. E_{tot} is the total energy relative to that of C_{60}. E_{coh} is the cohesion energy. AR is the average radius of carbon cage. The units of E_{coh} and AR are eV/atom and Å, respectively, all other units are eV.

n	MSI	E_{tot}	E_{coh}	HOMO	LUMO	gap	AR
0	0	0.00	−7.483	−5.22	−3.58	1.64	3.552
1	1	1.34	−7.431	−3.90	−3.64	0.26	3.548
2	1,7	2.32	−7.386	−4.33	−3.68	0.64	3.544
3	1,41,48	3.43	−7.338	−3.67	−3.67	0.00	3.539
4	1,7,28,35	4.46	−7.292	−4.12	−3.66	0.45	3.536
5	1, 7, 29, 34, 59	5.55	−7.244	−3.77	−3.03	0.74	3.531
6	1, 7, 28, 34, 37, 56	6.51	−7.199	−4.06	−3.22	0.84	3.527
7	1, 7, 15, 32, 35, 45, 57	7.94	−7.146	−3.50	−3.04	0.46	3.524
8	1, 7, 16, 19, 31, 36, 45, 57	9.21	−7.096	−3.85	−3.12	0.74	3.520
9	1, 7, 14, 17, 26, 44, 47, 52, 55	10.67	−7.042	−3.43	−2.89	0.54	3.517
10	1, 7, 14, 17, 26, 35, 44, 47, 54, 60	11.92	−6.993	−3.73	−2.98	0.75	3.514
11	1, 6, 11, 18, 23, 27, 33, 40, 48, 51, 58	13.49	−6.937	−3.31	−2.71	0.60	3.511
12	1, 6, 11, 16, 18, 26, 36, 44, 46, 49, 54, 60	14.59	−6.890	−3.95	−2.59	1.36	3.507

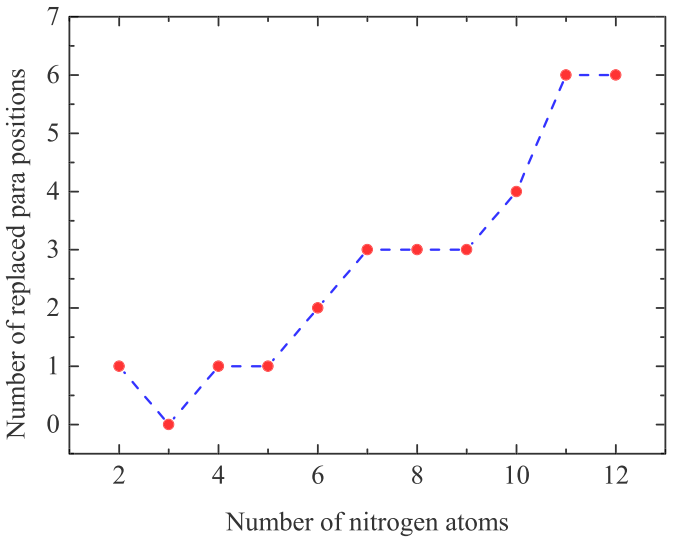

Fig. 9. Number of nitrogen-substituted para positions of the most stable structures of $C_{60-n}N_n$ (n = 2–12). (A colour version of this figure can be viewed online.)

heterofullerenes with more than 9 nitrogen atoms, we have proposed a classification method to filter the isomers with special substructures, enhancing the screening efficiency significantly. For $C_{48}N_{12}$, we obtain the Hultman's and Manaa's structures and other 24 low-lying isomers whose stabilities are between these two structures. All the most stable structures we obtained, except $C_{58}N_2$ and $C_{48}N_{12}$, have higher stabilities than those of the ones reported in literatures so far. The substituted para positions are dominant to the stabilities of azafullerenes, since in all the obtained most stable structures, the number of substituted para positions increases with higher nitrogen concentration.

The vibrational calculations confirm that all the obtained low energy structures are stable. For these stable structures, temperature makes no effect on their stability ranking, so the most stable structure always keeps the highest stability in the temperature range of 0–300 K. Compared to neutral molecules, the most stable anions and cations usually have different structures. For various charge states, the most stable structures always prefer minimal spin multiplicities. Our finding will provide theoretical foundations to generate experimental interest of heterofullerenes, which might help to further explore the potential applications with these nanostructures.

Acknowledgments

This work was supported by the National Natural Science Foundation of China (Grant Nos. 11474100, U1601212, 11574088 and 51675494), the Open Research Fund Program of the State Key Laboratory of Low-Dimensional Quantum Physics (Grant No. KF201809), the Guangdong Natural Science Funds for Distinguished Young Scholars (Grant No. 2014A030306024), and the Fundamental Research Funds for the Central Universities (No. 2018ZD46). The computer times at National Supercomputing Center in Guangzhou (NSCCGZ) and Guangzhou Ginpie Technology are gratefully acknowledged.

Appendix A. Supplementary data

See supplementary information for the 2-body interactions, some examples for the classification method, the energy information of all the calculated $C_{48}N_{12}$ isomers, the structural details of the 24 obtained remarkably stable isomers of $C_{48}N_{12}$, the calculation results of charged azafullerenes and more plots of the GFE versus temperature by vibrational calculations.

Supplementary data to this article can be found online at https://doi.org/10.1016/j.carbon.2019.07.086.

References

[1] H.R. Karfunkel, T. Dressler, A. Hirsch, Heterofullerenes: structure and property predictions, possible uses and synthesis proposals, J. Comput. Aided Mol. Des. 6 (1992) 521–535.
[2] E. David, An overview of advanced materials for hydrogen storage, J. Mater. Process. Technol. 162–163 (2005) 169–177.
[3] J. Lan, D. Cao, W. Wang, $Li_{12}Si_{60}H_{60}$ fullerene composite: a promising hydrogen storage medium, ACS Nano 3 (2009) 3294–3300.
[4] H. Liu, J.W. Chen, Nonlinear optical properties of a new substituted cluster: $C_{48}N_{12}$, Physica Status Solidi B-Basic Research 237 (2003) 575–580.
[5] X. Zhou, W.-Q. Li, B. Shao, W.Q. Tian, Nonlinear optical properties of fullerene C_{96} (D_{3d}) and related heterofullerenes, J. Phys. Chem. C 117 (2013) 23172–23177.
[6] Z. Jin, Z. Changgan, C. Xin, W. Kedong, W. Guanwu, W. Jinlong, J.G. Hou, Z. Qingshi, Single $C_{59}N$ molecule as a molecular rectifier, Phys. Rev. Lett. 95 (2005), 045502/045501-045504.
[7] G. Rotas, N. Tagmatarchis, Azafullerene $C_{59}N$ in donor-acceptor Dyads: synthetic approaches and properties, Chem. Eur. J. 22 (2016) 1206–1214.
[8] T. Guo, C. Jin, R.E. Smalley, Doping bucky: formation and properties of boron-doped buckminsterfullerene, J. Phys. Chem. 95 (1991) 4948–4950.
[9] T. Pradeep, V. Vijayakrishnan, A.K. Santra, C.N.R. Rao, Interaction of nitrogen with fullerenes: nitrogen derivatives of C_{60} and C_{70}, J. Phys. Chem. 95 (1991) 10564–10565.
[10] J.F. Christian, Z. Wan, S.L. Anderson, Nitrogen ion $N^+ + C_{60}$ fullerene reactive scattering: substitution, charge transfer, and fragmentation, J. Phys. Chem. 96 (1992) 10597–10600.
[11] H.-J. Muhr, R. Nesper, B. Schnyder, R. Kötz, The boron heterofullerenes $C_{59}B$ and $C_{69}B$: generation, extraction, mass spectrometric and XPS characterization, Chem. Phys. Lett. 249 (1996) 399–405.
[12] D.E. Clemmer, J.M. Hunter, K.B. Shelimov, M.F. Jarrold, Physical and chemical evidence for metallofullerenes with metal atoms as part of the cage, Nature 372 (1994) 248.
[13] J.C. Hummelen, B. Knight, J. Pavlovich, R. Gonzalez, F. Wudl, Isolation of the heterofullerene $C_{59}N$ as its dimer $(C_{59}N)_2$, Science 269 (1995) 1554–1556.
[14] O. Vostrowsky, A. Hirsch, Heterofullerenes, Chemical Reviews 106 (2006) 5191–5207.
[15] L. Hultman, S. Stafstrom, Z. Czigany, J. Neidhardt, N. Hellgren, I.F. Brunell, K. Suenaga, C. Colliex, Cross-linked nano-onions of carbon nitride in the solid phase: existence of a novel $C_{48}N_{12}$ aza-fullerene, Phys. Rev. Lett. 87 (2001), 225503.
[16] F.A. Shakib, M.R. Momeni, Isolation: a strategy for obtaining highly doped heterofullerenes, Chem. Phys. Lett. 514 (2011) 321–324.
[17] K. Srinivasu, N.K. Jena, S.K. Ghosh, Electronic structure, stability and nonlinear optical properties of aza-fullerenes $C_{60-2n}N_{2n}$(n=1–12), AIP Adv. 2 (2012), 042111.
[18] Z.F. Chen, X.Z. Zhao, A.C. Tang, Theoretical studies of the substitution patterns in heterofullerenes $C_{60-x}N_x$ and $C_{60-x}B_x$ (x=2-8), J. Phys. Chem. A 103 (1999) 10961–10968.
[19] Z. Chen, U. Reuther, A. Hirsch, W. Thiel, Theoretical studies on the substitution patterns in heterofullerenes $C_{70-x}N_x$ and $C_{70-x}B_x$ (x = 2–10), J. Phys. Chem. A 105 (2001) 8105–8110.
[20] H. Sharma, I. Garg, K. Dharamvir, V.K. Jindal, Structural, electronic, and vibrational properties of $C_{60-n}N_n$ (n=1-12), J. Phys. Chem. A 113 (2009) 9002–9013.
[21] I. Garg, H. Sharma, K. Dharamvir, V.K. Jindal, Substitutional patterns in boron doped heterofullerenes $C_{60-n}B_n$ (n = 1-12), J. Comput. Theor. Nanosci. 8 (2011) 642–655.
[22] B. Brena, Y. Luo, Electronic structures of azafullerene $C_{48}N_{12}$, J. Chem. Phys. 119 (2003) 7139–7144.
[23] Z.F. Chen, H.J. Jiao, D. Moran, A. Hirsch, W. Thiel, P.V. Schleyer, Aromatic stabilization in heterofullerenes $C_{48}X_{12}$ (X = N, P, B, Si), J. Phys. Org. Chem. 16 (2003) 726–730.
[24] M.R. Manaa, $C_{48}N_{12}$ and $C_{48}B_{12}$ as a donor-acceptor pair for molecular electronics, Chem. Phys. Lett. 382 (2003) 194–197.
[25] M.R. Manaa, H.A. Ichord, D.W. Sprehn, Predicted molecular structure of novel $C_{48}B_{12}$, Chem. Phys. Lett. 378 (2003) 449–455.
[26] M.R. Manaa, D.W. Sprehn, H.A. Ichord, High-energy structures of azafullerene $C_{48}N_{12}$, Chem. Phys. Lett. 374 (2003) 405–409.
[27] B. Schimmelpfennig, H. Agren, S. Csillag, Theoretical ^{13}C and ^{15}N NMR spectra for the $C_{48}N_{12}$ azafullerene, Synth. Met. 132 (2003) 265–268.
[28] R.H. Xie, G.W. Bryant, V.H. Smith, Raman scattering in C_{60} and $C_{48}N_{12}$ azafullerene: first-principles study, Phys. Rev. B 67 (2003).
[29] R.H. Xie, G.W. Bryant, V.H. Smith, Electronic, vibrational and magnetic properties of a novel $C_{48}N_{12}$ aza-fullerene, Chem. Phys. Lett. 368 (2003) 486–494.
[30] R.H. Xie, L. Jensen, G.W. Bryant, J.J. Zhao, V.H. Smith, Structural, electronic, and

magnetic properties of heterofullerene $C_{48}B_{12}$, Chem. Phys. Lett. 375 (2003) 445–451.
[31] E. Emanuele, F. Negri, G. Orlandi, Computed electronic and vibrational spectra of the most stable isomers of $C_{48}N_{12}$ azafullerene, Chem. Phys. 306 (2004) 315–324.
[32] S. Stafstrom, L. Hultman, N. Hellgren, Predicted stability of a new aza[60] fullerene molecule, $C_{48}N_{12}$, Chem. Phys. Lett. 340 (2001) 227–231.
[33] M.R. Manaa, D.W. Sprehn, H.A. Ichord, Prediction of extended aromaticity for a novel $C_{48}N_{12}$ azafullerene structure, J. Am. Chem. Soc. 124 (2002) 13990–13991.
[34] N. Kurita, K. Kobayashi, H. Kumahora, K. Tago, Bonding and electronic properties of substituted fullerenes $C_{58}B_2$ and $C_{58}N_2$, Phys. Rev. B 48 (1993) 4850–4854.
[35] S. Mohr, P. Pochet, M. Amsler, B. Schaefer, A. Sadeghi, L. Genovese, S. Goedecker, Boron aggregation in the ground states of boron-carbon fullerenes, Phys. Rev. B (2014) 89.
[36] K. Balasubramanian, Enumeration of chiral and positional isomers of substituted fullerene cages (C_{20}-C_{70}), J. Phys. Chem. 97 (1993) 6990–6998.
[37] S. Soleimani-Amiri, M. Koohi, Structure, topology, vibrational frequency, frontier molecular orbital gaps, stability, charge, NICS, and conductivity of non-segregated silicon heterofullerenes: a DFT approach, in: M. Yu, Z.K. Weng (Eds.), 2018 Ieee International Conference on Manipulation, Manufacturing and Measurement on the Nanoscale, 2018, pp. 51–54.
[38] M. Matsubara, C. Massobrio, Stability of charged Si-doped heterofullerenes: a first-principles molecular dynamics study, Phys. Rev. B (2009) 79.
[39] J.-J. Adjizian, A. Vlandas, J. Rio, J.-C. Charlier, C.P. Ewels, Ab Initio Infrared Vibrational Modes for Neutral and Charged Small Fullerenes (C_{20}, C_{24}, C_{26}, C_{28}, C_{30} and C_{60}), Philosophical Transactions of the Royal Society a-Mathematical Physical and Engineering Sciences, 2016, p. 374.
[40] Y. Wang, S. Diaz-Tendero, F. Martin, M. Alcami, Key structural motifs to predict the cage topology in endohedral metallofullerenes, J. Am. Chem. Soc. 138 (2016) 1551–1560.
[41] H.N. Vergara Reyes, E. Chigo Anota, M. Castro, C_{60}-like boron carbide and carbon nitride fullerenes: stability and electronic properties obtained by DFT methods, Fullerenes, Nanotub. Carbon Nanostruct. 26 (2018) 52–60.
[42] A. Rodriguez Juarez, F. Ortiz-Chi, M. Borges-Martinez, G. Cardenas-Jiron, M. Salazar Villanueva, E. Chigo Anota, Stability, electronic and optical properties of the boron nitride cage ($B_{47}N_{53}$) from quantum mechanical calculations, Phys. E Low-dimens. Syst. Nanostruct. 111 (2019) 118–126.
[43] G. Kresse, J. Hafner, Ab initio molecular dynamics for liquid metals, Phys. Rev. B 47 (1993) 558–561.
[44] G. Kresse, J. Furthmüller, Efficient iterative schemes for ab initio total-energy calculations using a plane-wave basis set, Phys. Rev. B 54 (1996) 11169–11186.
[45] G. Kresse, J. Furthmüller, Efficiency of ab-initio total energy calculations for metals and semiconductors using a plane-wave basis set, Comput. Mater. Sci. 6 (1996) 15–50.
[46] G. Kresse, D. Joubert, From ultrasoft pseudopotentials to the projector augmented-wave method, Phys. Rev. B 59 (1999) 1758–1775.
[47] J.P. Perdew, K. Burke, M. Ernzerhof, Generalized gradient approximation made simple, Phys. Rev. Lett. 77 (1996) 3865–3868.
[48] Z.-Q. Fan, Z.-H. Zhang, X.-Q. Deng, G.-P. Tang, H.-L. Zhu, Y. Ren, F. Xie, Structural, electronic, and transport properties of I_h-symmetry-breaking C_{60} isomers, Comput. Mater. Sci. 91 (2014) 15–19.
[49] N. Kurita, K. Kobayashi, H. Kumahora, K. Tago, K. Ozawa, Molecular structures, binding energies and electronic properties of dopyballs $C_{59}X$ (X=B, N and S), Chem. Phys. Lett. 198 (1992) 95–99.
[50] F. Chen, D. Singh, S.A. Jansen, Electronic effects in metal complexation of fullerenes C_{60}, $C_{59}N$, and $C_{59}B$, J. Phys. Chem. 97 (1993) 10958–10963.
[51] W. Powell, F. Cozzi, G. Moss, C. Thilgen, R.-R. Hwu, A. Yerin, Nomenclature for the C_{60}-I_h and C_{70}-$D_{5h\ (6)}$ fullerenes (IUPAC recommendations 2002), Pure Appl. Chem. 74 (2002) 629–695.
[52] Y.-H. Cheng, J.-H. Liao, Y.-J. Zhao, X.-B. Yang, An extended cluster expansion for ground states of heterofullerenes, Sci. Rep. 7 (2017) 16211.
[53] P. Wurfel, The chemical potential of radiation, J. Phys. C Solid State Phys. 15 (1982) 3967.
[54] P.H. Acioli, J. Jellinek, Electron binding energies of anionic magnesium clusters and the nonmetal-to-metal transition, Phys. Rev. Lett. 89 (2002) 213402.
[55] J. Tamuliene, Electronic and vibrational spectra of C_{60} and its ions, Fullerenes, Nanotub. Carbon Nanostruct. 23 (2015) 187–195.
[56] A.K. Kandalam, R. Pandey, M. Blanco, A. Costales, J. Recio, J.M. Newsam, First principles study of polyatomic clusters of AlN, GaN, and InN. 1. Structure, stability, vibrations, and ionization, J. Phys. Chem. B 104 (2000) 4361–4367.
[57] T. Baruah, M.R. Pederson, R.R. Zope, Vibrational stability and electronic structure of a B_{80} fullerene, Phys. Rev. B 78 (2008), 045408.
[58] D. Dragoni, T.D. Daff, G. Csányi, N. Marzari, Achieving DFT accuracy with a machine-learning interatomic potential: thermomechanics and defects in bcc ferromagnetic iron, Physical Review Materials 2 (2018), 013808.
[59] T.P. Martin, Alkali halide clusters and microcrystals, Phys. Rep. 95 (1983) 167–199.
[60] S. Yang, F. Liu, C. Chen, M. Jiao, T. Wei, Fullerenes encaging metal clusters-clusterfullerenes, Chem. Commun. 47 (2011) 11822–11839.